Available online at www.sciencedirect.com
ScienceDirect
Trans. Nonferrous Met. Soc. China 25(2015) 3315−3322
Transactions of Nonferrous Metals Society of China
www.tnmsc.cn

In situ laser deposition of NiTi intermetallics for corrosion improvement of Ti−6Al−4V alloy

M. N. MOKGALAKA[1,2], A. P. I. POPOOLA[1], S. L. PITYANA[1,2]

1. Department of Chemical, Metallurgical and Materials Engineering, Tshwane University of Technology, Pretoria 0001, South Africa;
2. Council for Scientific and Industrial Research, National Laser Centre, Pretoria 0001, South Africa

Received 5 September 2014; accepted 29 June 2015

Abstract: NiTi intermetallic coatings were fabricated on the surface of Ti−6Al−4V alloy by melting Ni and Ti powders using laser metal deposition (LMD) process. The effects of NiTi reinforcement content on the microstructure, hardness and corrosion properties of the coatings were examined. The results show that the deposited coatings are characterized by NiTi, $NiTi_2$ and $NiTi_3$ intermetallic phases. An appreciable increase in corrosion resistance is obtained for all the coatings, and Ti55Ni45 coating shows the highest corrosion resistance; while coatings Ti50Ni50 and Ti45Ni55 follow in that succession. The reinforcement materials are proven to be corrosion resistant in the tested environment, and the effect of Ti is more dominant.
Key words: Ti−6Al−4V alloy; NiTi intermetallic; laser metal deposition; corrosion behaviour

1 Introduction

Ti−6Al−4V alloy is considered a capable structural material for aerospace, biomedical and petrochemical industries due to the combination of outstanding high specific strength, biocompatibility and good corrosion resistance [1]. However, due to the potential difference of the α+β phase of the alloy, galvanic interaction increases and acts as preferential sites for corrosion. Furthermore, the vanadium oxide that forms on the surface is insoluble in aqueous solution. Hence, the deterioration in the corrosion behaviour of Ti−6Al−4V alloy is evident [2]. As a result, their applications are restricted in severe corrosive environments.

Numerous studies with the purpose of improving the surface properties of Ti−6Al−4V alloy have been undertaken with different degrees of success. Researchers agree that changing the nature of the surface by using different surface engineering techniques is the best solution to overcome the limitation of titanium alloys [3,4]. Laser processing techniques have been found to be free from these shortcomings and can be used to enhance the surface properties of ferrous and non-ferrous metal surfaces [5−9]. As a flexible process, laser surface technique is used in the fabrication of different coatings for improving the surface properties and the repair of the worn parts [10]. Among the laser surface coating methods, laser deposition is the preferred method because of the novel microstructures and phases that can be formed due to rapid cooling and solidification rates associated with the processing technique [11]. Coatings generally have such microstructures that cannot be easily obtained by conventional techniques. One of the advantages of laser surface coating is that quite a number of metallic powders can be used to form intermetallic compounds exhibiting excellent wear resistance, good corrosion and oxidation resistance properties.

NiTi coatings have been a subject of great interest and have been widely exploited for a range of applications including aerospace, biomedical engineering and micro electrochemical system due to the above mentioned advantageous properties [12−16]. Many metals including stainless steel, aluminium and copper surfaces have been coated with NiTi to enhance their mechanical properties and corrosion resistance using laser deposition techniques, plasma transfer arc (PTA), plasma welding, plasma spray coating and sputtering process, all with different degrees of successes [17−20].

Corresponding author: A. P. I. POPOOLA; Tel: +27-123823513; E-mail: popoolaapi@tut.ac.za; spityana@csir.co.za
DOI: 10.1016/S1003-6326(15)63989-9

Among the wide research conducted in surface modification of Ti−6Al−4V, the focus has been on the microstructural evolution, improved hardness and wear resistance, with little on improving corrosion resistance. According to the available information in the open literature, there is no research on laser deposition of NiTi on Ti−6Al−4V alloy. In this work, mechanically alloyed Ni and Ti elemental powders were used to form in situ NiTi intermetallic — thin surface coatings on the Ti−6Al−4V substrate. The laser metal deposition technique was employed to melt powders of different compositions: Ti50Ni50, Ti45Ni55 and Ti55Ni45. The microstructure, phase composition, microhardness and corrosion properties of the coatings were investigated.

2 Experimental

2.1 Materials

The materials used in the experiment are elemental Ni and Ti powders with the particle size fraction within the range from 45 to 63 μm. Prior to milling, the powders were weighed and mixed together to give nominal compositions of Ti55Ni45, Ti50Ni50 and Ti45Ni55 (mass fraction, %). The initially mixed powders were mechanically alloyed in a planetary ball mill by subjecting the particles to repeated welding, fracturing and re-welding from the collision of the particles and the grinding medium. The milling was performed for 2 h to allow the powders to reach a steady state where homogeneous NiTi powder was produced. The ball to powder ratio was kept uniform at 10:1 and the rotation speed was 300 r/min.

2.2 Laser surface coating

The cold rolled Ti−6Al−4V plate with dimensions of 72 mm × 72 mm × 5 mm was used as the substrate for depositing the coatings. The plates were sandblasted and cleaned with acetone prior to the laser coating process. Table 1 shows the laser experimental processing parameters of the coating deposition. The free flowing NiTi pre-alloyed was fed through a three-way nozzle with argon shielding gas stream. The argon gas flow rate was 5 L/min. The CW 4.4 kW Rofin Sinar Nd: YAG laser operated with 1.064 μm in wavelength was used to deposit the coatings. The beam spot on the target was 2 mm in diameter. The scanning speed, laser power and the powder flow rate were kept constant.

2.3 Microhardness analysis

The Vickers hardness of polished specimens was determined using a Matsuzawa Seiko Vickers microhardness tester (model MHT−1) with a Vickers diamond indenter. An indenting load of 100 g, a spacing of 50 μm and a dwell time of 10 s were used for each hardness indent action. Indentations were made across the deposited layer in three areas from the top of a clad into the substrate. The Vickers hardness was calculated using the equation:

$$H_{\mathrm{HV}} = 1.854\frac{F}{S} \tag{1}$$

where F is the applied load (kg) and S is the area of the indentation (mm^2).

2.4 Corrosion analysis

The electrochemical corrosion test was conducted using potentiodynamic polarisation technique equipped with potentiostat Autolab type 3 according to ASTM G3−89 and ASTM 5−94 standards in 3.5% NaCl solution. A three-electrode arrangement, with an electrode containing Ag/AgCl 3 mol/L KCl as the reference electrode (SCE) was used. The electrochemical corrosion behaviour of the samples was investigated using linear polarization. The analysis was carried out at a scan rate of 0.111 m/s, a start potential of −1.5 V and a stop potential of +1.5 V for a duration of 1 h.

2.5 Characterization of materials

The metallographic samples were sectioned with a Corundum L205 cut-off wheel using a Struers Discotom−2 cutting machine. After sectioning, the specimens were hot-mounted in clear thermosetting Bakelite resin. The specimens were then ground and polished to a 0.04 μm (OP-S suspension) surface finish with a Struers TegraForce−5 auto/manual polisher and etched in Kroll reagent by immersing the samples for approximately 10 s. The microstructure was characterized on an Olympus BX51M optical microscope and a Jeol JSM 6510 scanning electron microscope (SEM) equipped with energy dispersive spectroscopy (EDS). X-ray diffraction (XRD) was conducted using the Rigaku/Dmax 2200 PC automatic X-ray diffractometer with Cu target K_α radiation for phase identification.

Table 1 Laser experimental processing parameters for coating deposition

Composition	Laser power/W	Beam spot diameter/mm	Scanning speed/ ($mm \cdot s^{-1}$)	Powder feed rate/ ($g \cdot min^{-1}$)	Carrier and shield gas	Gas flow rate/ ($L \cdot min^{-1}$)
Ti45Ni55 Ti50Ni50 Ti55Ni45	800	2	8	3	Argon	5

3 Results and discussion

3.1 Microstructural analysis of coatings

3.1.1 Ti55Ni45 coating

The microstructural images of the cross section of the deposited Ti55Ni45 coating were taken at different places of interest on the coating to understand the morphology of the coatings and the distribution of NiTi within the coating. Figure 1 shows the micrographs of the Ti55Ni45 coating on Ti−6Al−4V substrate. The coating is characterized by three different phases distinguished by their appearance as indicated in Fig. 1(a). Uniform distribution of these phases was observed when going deeper into the coating as indicated in Fig. 1(b). The phases were identified as NiTi with brown colour, Ti-rich phase with white colour and a flower-like morphology in some areas and $NiTi_2$ was observed at grain boundary occurring with $NiTi_3$ in other areas of the coating. The overall elemental analysis of the coating revealed that the $NiTi_2$ phase is the major constituent of the coating, as indicated in Fig. 1(c) and Table 2. The NiTi phase is characterized by good toughness and ductility, making it an ideal candidate of which corrosion and oxidation resistances are service requirements. The $NiTi_2$ phase is characterized by good combination of ductility and high hardness owing to its FCC crystal structure. Hence, it is the preferred candidate for wear resistant materials [21].

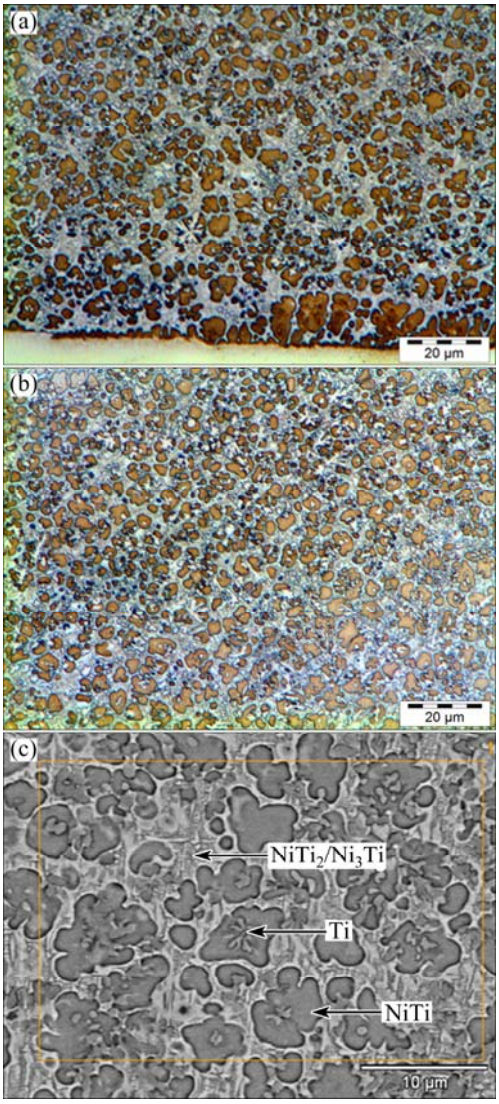

Fig. 1 Images of laser deposited Ti55Ni45/Ti−6Al−4V coatings: (a) Optical micrograph showing interface between coating and substrate; (b) Optical micrograph showing distribution of phases in coating; (c) SEM image for EDS analysis of coating

Table 2 EDS analysis of coatings (mole fraction, %)

C	Al	V	Ni	Ti
2.23	5.94	2.57	13.86	75.25

3.1.2 Ti50Ni50 coating

Figure 2(a) shows the cross section of the laser deposited Ti50Ni50 coating on the Ti−6Al−4V substrate with a thickness of 550 μm. The coating was characterized by good metallurgical bond between the substrate and the coating indicated by the absence of cracks or pores and low dilution rate. The coating also exhibited uniform distribution of the phases formed as a result of melting as shown in Fig. 2(b). Elemental analysis performed on the coating as presented in Fig. 2(c), revealed that the matrix consisting of NiTi phase and light phases (Ni_2Ti and Ni_3Ti) around the grain boundary was formed.

3.1.3 Ti45Ni55 coating

The optical micrographs and SEM image of the laser deposited Ni-rich Ti45Ni55 coating are shown in Fig. 3. The microstructure revealed good homogeneity with equiaxed grains, a dendritic structure and some primary dendrites and interdendritic matrix as shown in Fig. 3(b). The results of the EDS indicated that the primary dendrite which appeared as grey structures was NiTi and the connected interdendritic matrix occurring at grain boundaries is Ni_2Ti. The volume fraction of the $NiTi_2$ phase in the intermetallic could not be analytically determined. The phases formed in this matrix were similar to those reported by VERDIAN et al [22] during the characterization and evaluation of the corrosion behaviour of NiTi−Ti_2Ni−Ni_3Ti multiphase intermetallics produced by vacuum sintering. The volume fractions of the intermetallics in the sintered samples were reported to be 34% NiTi, 27% $NiTi_2$ and 39% Ni_3Ti.

3.2 X-ray diffraction analysis

3.2.1 Ti50Ni50 coating

The Ti50Ni50 coating (Fig. 4(a)) showed good combination of intermetallic phases as compared with other coatings. The main constituent of the coating was

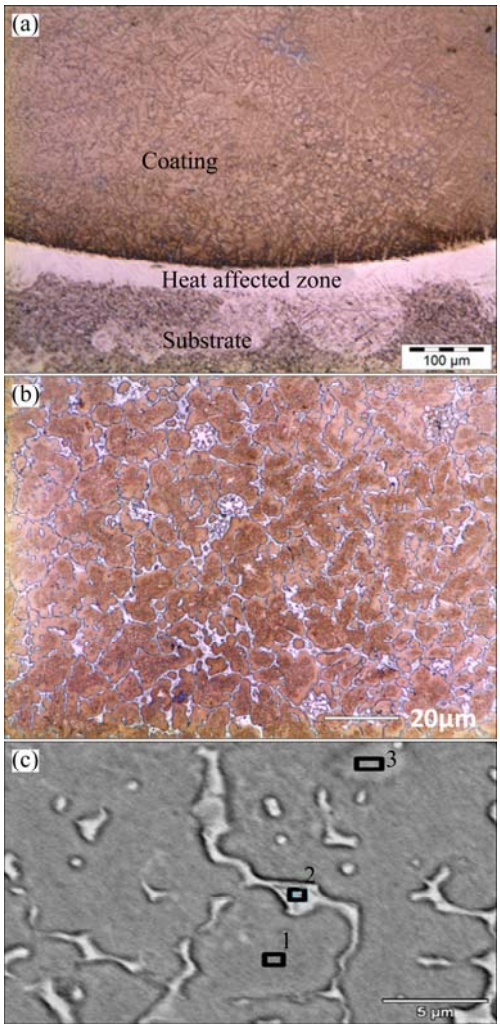

Area No.	Mole fraction/%						
	C	Al	V	N	O	Ni	Ti
1	7.07	5.87	2.64	9.98	7.00	4.54	62.88
2	7.84	4.6	4.09	0	0	20.97	62.46
3	12.66	7.19	2.72	0	0	6.17	71.14

Fig. 2 Images of laser deposited Ni50Ti50/Ti−6Al−4V coatings: (a) Optical micrograph showing interface between coating and substrate; (b) Optical micrograph showing uniform distribution of phases; (c) SEM image showing elemental analysis of phases at high magnification

the hard $NiTi_2$ and the ductile NiTi martensite phase with some traces of the soft austenite phase. The coatings revealed some weak peaks of Ni_3Ti phase characterized by brittle structure with no trace of TiO_2 as observed with other coatings. The combination of these phases alters good corrosive wear properties of the coatings.

3.2.2 Ti55Ni45 coating

It was observed that the Ti55Ni45 coating (Fig. 4(b)) presented a small amount of intermetallic phases, with the dominant phase being the Ti phase followed by the

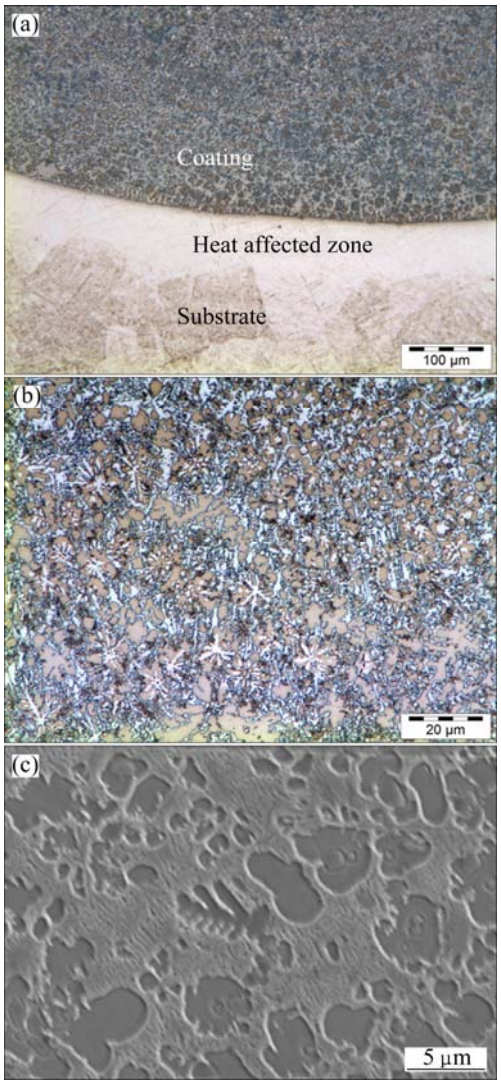

Fig. 3 Images of laser deposited Ti45Ni55 coatings on Ti−6Al−4V substrate: (a) Optical micrograph showing interface between coating and substrate; (b) Optical micrograph showing inter-connected matrix in coating; (c) SEM image showing high magnification of coating

$NiTi_2$ and Ni_3Ti. Due to many Ti phases, it is expected that the coatings will have high hardness which will improve the wear resistance. However, a few intermetallic phases and many Ti phases suggested that the distribution of the phases in the coating was non-uniform, which might lead to the formation of preferential sites for corrosion and wear. However, this was not the case as the coating presented high corrosion resistance compared with other coatings.

3.2.3 Ti45Ni55 coating

The Ti45Ni55 coating was characterized by Ti phase as the main constituent and an increased content of intermetallic phases ($NiTi−NiTi_2−NiTi_3$) with traces of TiO_2. For this coating, the soft $B'2$ austenite phase was not detected and the peaks of $NiTi_2$ phase were weak overlapping with the $NiTi_3$ phase. This suggested that the

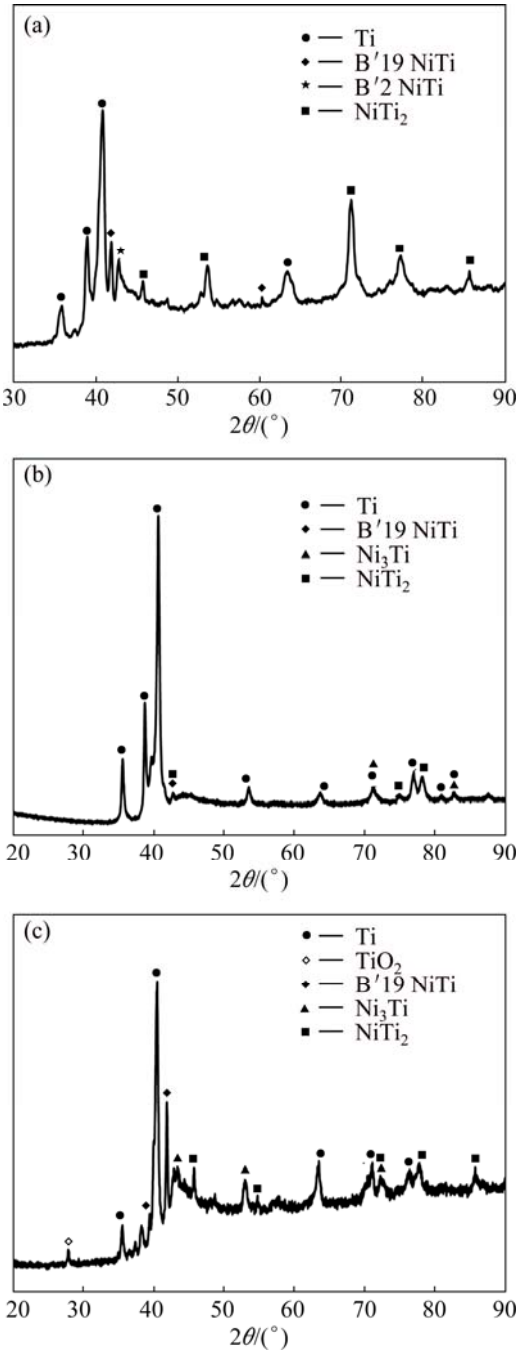

Fig. 4 XRD patterns of laser deposited NiTi coatings on Ti−6Al−4V substrate: (a) Ti50Ni50; (b) Ti55Ni45; (c) Ti45Ni55

coating was susceptible to corrosive wear shortcomings. The intermetallic phases identified by XRD analysis, were in accordance with the results obtained through EDS analysis presented in Section 3.1 under microstructural analysis.

3.3 Microhardness of coatings

The hardness profile across the depth of the NiTi intermetallic coating was measured by the Matsuzawa Seiko hardness tester with a load of 100 g, a spacing of 50 μm and a dwell time of 15 s. The hardness profiles of the deposited NiTi showing the hardness values in the coating, the heat affected zone and the substrate are presented in Fig. 5. Experimental results indicated that the surface hardness of the laser deposited NiTi coatings increased compared with the parent material Ti−6Al−4V alloy. High hardness in the deposited layer was attributed to the formation of the fine grain microstructure produced during melting and formation of the hard intermetallic phases. The Ti55Ni45 coating had the highest hardness values compared with Ti45Ni55 and Ti50Ni50 coatings and the substrate with the average value of HV 430 higher than that of Ti−6Al−4V substrate (HV 380). The high hardness displayed by the coating (HV 742) was a result of excessive amount of Ti powder that was well dispersed within the coating, resulting in increased volume of inert secondary phase $NiTi_2$ with high hardness but brittle microstructure. An improvement in hardness was calculated to be 95% compared with the substrate.

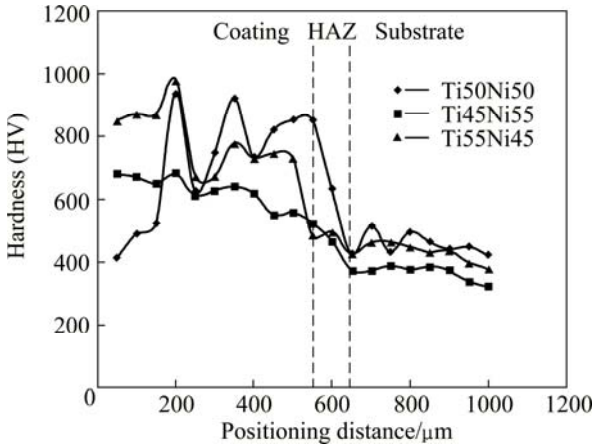

Fig. 5 Microhardness profiles of laser deposited coatings showing microhardness values of coating, heat affected zone and substrate

3.4 Corrosion behaviour analysis of coatings

Most titanium alloys have been reported to exhibit superior properties in contrast to the commercially pure (CP) titanium. Ti−6Al−4V alloy possesses advantageous properties because of the alloying elements. Coatings are used as protection against corrosion due to their ability to make inactive or less reactive surfaces of metals/alloys. Corrosion resistance usually arises because of surface oxide films mitigating against further corrosion reactions. Outstanding corrosion resistance of titanium alloys is a result of the highly stable, continuous, adherent and protective oxide film consisting of titanium dioxide (TiO_2) predominantly and also including aluminium oxide (Al_2O_3) and vanadium oxide (V_2O_5). However, the nature and the composition of the protective film depend on environmental conditions. The

degree of surface deterioration due to corrosion reactions also depends on the environment to a large extent. Passivation involves chemical resistance to the environments. The formed passive film can hinder the ingress of aggressive ions (from the environment) onto the metallic matrix and resist all potentials presented. Titanium and other elements on the periodic table are generally self-passivating elements. The Al and V in Ti−6Al−4V alloy make it prone to corrosion attack simply because of the breakdown of its passive film.

Table 3 shows the polarization data of the laser deposited NiTi coatings on Ti−6Al−4V substrate and the untreated Ti−6Al−4V substrate in 3.5% NaCl solution. The corrosion current density (J_{corr}), polarization resistance (R_p), corrosion potentials (φ_{corr}) and corrosion rate (CR) are extracted from the curves using Tafel extrapolation method and the data are listed in Table 3.

Table 3 Polarization data for laser deposited NiTi/Ti−6Al−4V coatings with substrate

Sample	φ_{corr}/V	J_{corr}/A	CR/(mm·year^{-1})	R_p/Ω
Ti−6Al−4V	−1.3211	5.28×10^{-3}	0.646671	60.90
Ti50Ni50	−0.9496	1.04×10^{-5}	0.017069	667.83
Ti55Ni45	−0.7503	3.15×10^{-6}	0.005161	1152.70
Ti45Ni55	−1.1024	2.23×10^{-5}	0.030721	446.16

From the polarization data obtained, the coatings exhibited an ideal passive behaviour, laid at lower current densities with a breakdown potential of 0.5 V as a result of the formation of a TiO_2 film on the surface. From the polarization graphs presented in Fig. 6, it could be observed that all the coatings experienced a positive shift in corrosion potential when compared with the Ti−6Al−4V substrate. An increase in corrosion potential of about 0.6 V was achieved as a result of laser deposition of NiTi. The corrosion current densities of all the deposited coatings were lower than those of the untreated Ti−6Al−4V substrate with corrosion potential slightly nobler. This is mainly because NiTi is nobler than Ti−6Al−4V, and corrosion attack will preferably take place in the substrate than in the coating. This is an indication that the coatings are more corrosion resistant than the Ti−6Al−4V substrate. The laser deposited NiTi intermetallic coatings on Ti−6Al−4V substrate present open circuit potentials higher than those of the Ti−6Al−4V substrate. The anodic reaction is controlled by the formation of strong intermetallic and stable oxides on the anodic sites while the cathodic reaction is controlled by the formation of hydroxyl ions (OH^-) on the cathode sites of the metal surface. Thus, it is clearly evident that the reaction is both anodically and cathodically controlled and this generally accounts for the synergistic effect [23].

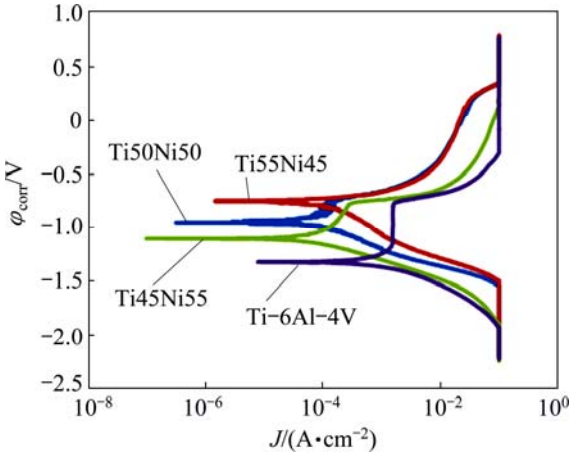

Fig. 6 Comparative polarization curves of laser-deposited NiTi/Ti−6Al−4V coatings with substrate in 3.5% NaCl solution

It is observed that polarization resistance of the deposited coatings is increased by approximately 10 times compared with that of the Ti−6Al−4V substrate. The corrosion rate on the other hand is two orders of magnitude lower than that of the Ti−6Al−4V substrate, indicating that all the coatings show an improved corrosion resistance with Ti55Ni45 being the best. Passivation is observed on all the coatings, but Ti55Ni45 only reveals slight passivation. Uniform distribution of the NiTi reinforcement can be seen in the microstructure of this coating, the interfaces are clean, and the grain boundaries show no sign of micro segregation and good homogeneity is displayed. Hence, better corrosion properties are displayed by the coatings.

The examination of the samples after corrosion tests indicates that there are preferential sites for corrosion. It is well known that the common susceptible sites for corrosion attack are inclusions, secondary phase precipitates, grain boundaries and processing defects such as pores and cracks. From the micrographs presented in Fig. 7, it is observed that the coatings are free from processing defects and the sites that hasten corrosion are as a result of NaCl solution used during corrosion analysis. The defects act as locations where the protective film is defective and breakdown becomes easier in aggressive environments. Figure 7 presents the SEM images of the coatings after corrosion analysis. The coatings exhibit the typical passive region, with the passivity related to the formation of TiO_2 and NiO passive films; however, the presence of micro-cracks and non-uniform distribution of phases within the coating hinder the formation of the passive film, thus deteriorating the corrosion resistance behaviour.

The typical morphologies are shown in Fig. 7, representing the substrate material and all the coatings

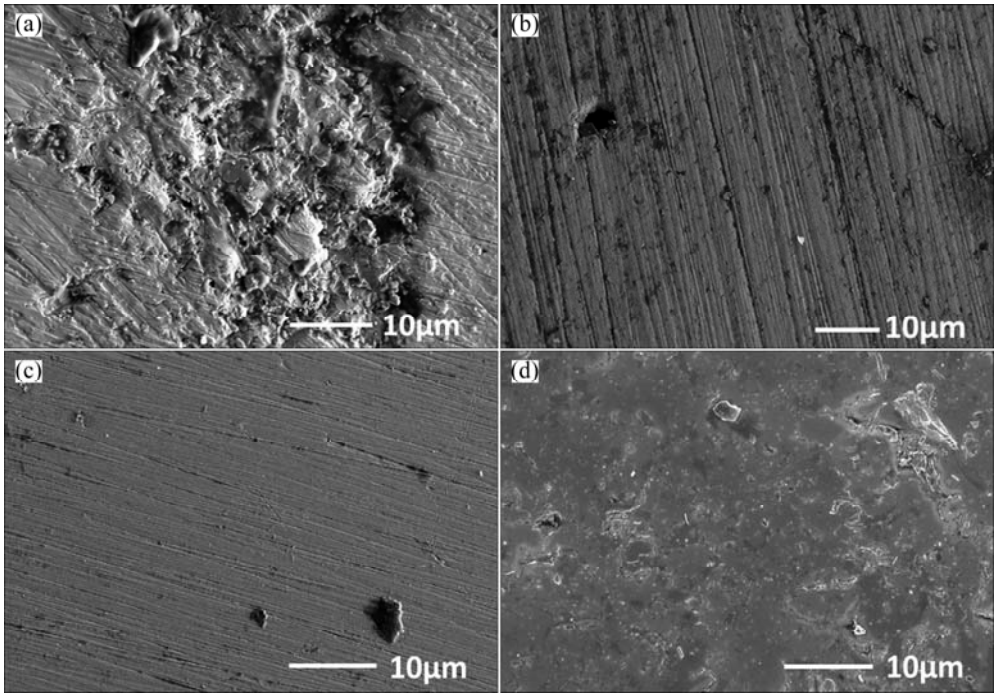

Fig. 7 SEM images of all corroded samples immersed in 3.5% NaCl solution: (a) Ti−6Al−4V substrate; (b) Ti50Ni50; (c) Ti55Ni45; (d) Ti45Ni55

developed. In Fig. 7(b), for Ti50Ni50 coating, it is observed that the coating is attacked by pitting primarily on the surface when the electrolyte reaches the surface. Similarly, on the surface of Ti55Ni45 coatings as indicated in Fig. 7(c), physical examination reveals that this coating resists corrosion better than other coatings and substrate. However, the electrolyte does not reach the substrate as there are no cracks or pores to act as preferential sites for corrosion reactions. Aggressive pitting attack is observed in Fig. 7(d), with slight deterioration. Comparing all coatings with the substrate, it is seen that the coatings resist corrosion attack better than the substrate, which is attributed to the chemical stability and strong inter atomic bonds due to inherent intermetallic phases formed as a result of in situ laser powder deposition.

4 Conclusions

1) Laser melting of Ni and Ti powders results in the formation of NiTi, $NiTi_2$ and $NiTi_3$ intermetallic phases that improve the properties of Ti−6Al−4V substrate.

2) A 95% increase in hardness is achieved with the coating that shows high corrosion resistance, exhibiting hardness value of HV 742 compared with HV 380 of the substrate.

3) An appreciable increase in corrosion resistance is accomplished. The sample with Ti55Ni45 coating shows the highest corrosion resistance; while Ti50Ni50 and Ti45Ni55 follow in that succession. Although the Ni content contributes to the improvement of corrosion resistance, the effect of Ti is more dominant.

Acknowledgement

This material is based upon work financially supported by the National Research Foundation, South Africa. The National Laser Centre, CSIR, Pretoria, South Africa is appreciated for laser facility. The authors acknowledge the support from Tshwane University of Technology, Pretoria, South Africa.

References

[1] SAVALANI M M, NG C C, LI Q H, MAN H C. In situ formation of titanium carbide using titanium and carbon nanotube powders by laser cladding [J]. Applied Surface Science, 2012, 258(7): 3173−3177.

[2] ATAPOUR M, FATHI M H, SHAMANIAN M. Corrosion behaviour of Ti−6Al−4V alloy weldment in hydrochloric acid [J]. Journal of Materials and Corrosion, 2012, 63(2): 134−139.

[3] SREEDHAR C G., KRISHNAN S, GOKULARATHNAM C V, KRISHNAMURPHY R. Advances in physical metallurgy [J]. Journal of Materials Processing Technology, 2011, 114: 246−251.

[4] YETIM A F, YILDIZ F, VANGOLU Y, ALSARAN A, CELIK A. Several plasma diffusion process for improving wear properties of Ti6Al4V alloy [J]. Wear, 2009, 267(12): 2179−2185.

[5] DAI J J, HOU S Q. Laser gas nitriding of titanium and titanium alloys [J]. Surface Review and Letters, 2009, 16(6): 789−796.

[6] TIAN Y S, CHEN C Z, WANG D Y, LEI T Q. Laser surface modification of titanium alloys [J]. Surface Review and Letters, 2005, 12(1): 123−130.

[7] MAJUMDAR J D, MANNA I. Laser material processing [J].

International Materials Reviews, 2011, 56(5−6): 341−388.
[8] POPOOLA A P I, PITYANA S L, POPOOLA O M. Laser deposition of (Cu+Mo) alloying reinforcements on AA1200 substrate for corrosion improvement [J]. International Journal of Electrochemical Science, 2011, 6: 5038−5051.
[9] RAKHES M, KOROLEVA E, LIU Z. Improvement of corrosion performance of HVOF +MMC coating by laser surface treatment [J]. Journal of Surface Engineering, 2011, 27(10): 729−733.
[10] SUN Y, HAO M. Statistical analysis and optimization of process parameters in Ti6Al4V laser cladding using Nd:YAG laser [J]. Optics and Lasers in Engineering, 2012, 50(7): 985−995.
[11] TOYSERKANI E, KHAJEROUR A, CORBIN S. Laser cladding [M]. London: CRC Press, 2005.
[12] SUN S, DURANDET Y, BRANDT M. Parametric investigation of pulsed Nd:YAG laser cladding of stellite 6 on stainless steel [J]. Surface and Coatings Technology, 2005, 194(2): 225−231.
[13] MUDALI U K, KAUL R, NINGSHEN S, GANESH P, NATH A K, KHATAK H S, RAJ B. Influence of laser surface alloying with chromium and nickel on corrosion resistance of type 304L stainless steel [J]. Materials Science and Technology, 2006, 22(10): 1185−1192.
[14] HIRAGA H, INOUE T, SHIMURA H, MATSUNAWA A. Cavitation erosion mechanism of NiTi coatings made by laser plasma hybrid spraying [J]. Wear, 1999, 231(2): 272−278.
[15] SALEHI M, KARIMZADEH F, TAHVILIAN A. Formation of Ti–Ni intermetallic coatings on carbon tool steel by a duplex process [J]. Surface and Coatings Technology, 2001, 148(1): 55−60.
[16] ALLAFI J K, REN X, EGGELER G. The mechanism of multistage martensitic transformations in aged Ni-rich NiTi shape memory alloys [J]. Acta Materialia, 2002, 50(4): 793−803.
[17] SCHAUER J C, WINTER J. Plasma deposition of elastic wear resistant Si−C coatings on nickel−titanium for biomedical applications [J]. Journal of Applied Physics, 2008, 103(11): 113302.
[18] GERKE L, STELLA J, SCHAUER J C, POHL M, WINTER J. Cavitation erosion resistance of a C:H coatings produced by PECVD on stainless steel and NiTi substrates [J]. Surface and Coatings Technology, 2010, 204: 3418−3424.
[19] ABUBAKAR T, RAHMAN M, DOWLING D P, STOKES J, HASHMI M S J. Adhesion performance of TiN coating with amorphous NiTi alloy interlayer onto 316 stainless steel deposited by sputtering process [J]. Surface Engineering, 2010, 26: 499−505.
[20] BRAM M, AHMAD-KHANLOU A, BUCHKREMER H P, TOVER D. Vacuum plasma spraying of NiTi protection layers [J]. Materials Letters, 2002, 57: 647−651.
[21] GAO F, WANG H M. Dry sliding wear property of a laser melting/deposited Ti_2Ni/TiNi intermetallic alloy [J]. Intermetallics, 2008, 16(2): 202−208.
[22] VERDIAN M M, RAEISSI K, SALEHI M, SABOONI S. Characterization and corrosion behaviour of NiTi−Ti_2Ni−Ni_3Ti multiphase intermetallics produced by vacuum sintering [J]. Vacuum 2011, 86: 91−95.
[23] JOSEPH R X, RAJENDRAN S N. Corrosion inhibition effect of substituted thiadiazoles on brass [J]. International Journal of Electrochemical Science, 2011, 6(2): 348−366.

原位激光沉积 NiTi 涂层 提高 Ti−6Al−4V 合金的耐腐蚀性能

M. N. MOKGALAKA[1,2], A. P. I. POPOOLA[1], S. L. PITYANA[1,2]

1. Department of Chemical, Metallurgical and Materials Engineering, Tshwane University of Technology, Pretoria 0001, South Africa;
2. Council for Scientific and Industrial Research, National Laser Centre, Pretoria 0001, South Africa

摘 要：采用激光金属沉积工艺通过熔化 Ni、Ti 粉末在 Ti−6Al−4V 合金表面沉积 NiTi 涂层。研究 NiTi 涂层含量对合金显微组织、硬度和耐蚀性能的影响。结果表明，涂层由 NiTi、$NiTi_2$ 和 $NiTi_3$ 相组成。含 NiTi 涂层的 Ti−6Al−4V 合金的耐腐蚀性能均得到一定程度的提高，且涂层成分为 Ti55N45 的 Ti−6Al−4V 合金的耐腐性能最好，其次为含 Ti50Ni50 和 Ti45Ni55 涂层的合金。在实验条件下，所有含 NiTi 涂层的材料具有良好的耐蚀性能，且 NiTi 中 Ti 元素的影响更加显著。

关键词：Ti−6Al−4V 合金；NiTi 金属间合物；激光金属沉积；腐蚀行为

(Edited by Wei-ping CHEN)